

Behavior of Three-Dimensionally Woven Glass Fiber Reinforced Polymeric Bridge Deck

by

Charles M. Johnson, NC State Univ. MS Student
Tarek S. Mohamed, NC State Univ. MS Student
Sami H. Rizkalla, NC State Univ. Distinguished Prof.

ABSTRACT

In the past two decades, glass fiber reinforced polymer (GFRP) bridge decks have been considered as an alternative to conventional steel and concrete bridge decking. The study presented in this paper investigated the behavior of a new and innovative 3-D woven GFRP bridge deck. The proposed deck consisted of two skins of E-glass fabric and vertical webs to act as flexural members supported by the girders. Each skin consisted of two orthogonal woven fabrics which were stitched together by fibers in the perpendicular direction to form a 3-D GFRP material for the entire cross section. Balsa cores were inserted to maintain the configuration of the cross section during the vacuum infusion process using epoxy resin. This paper focused on the behavior of two types of decks: GFRP bridge deck and GFRP-concrete hybrid deck. The fundamental material characteristics of the 3-D woven GFRP materials used, including the tension, flexure, and shear, are presented. The limit state behaviors of the two decks are discussed. A comparison of the behavior of the panels infused with vinyl ester and epoxy are presented. The paper discusses also the various type of shear connectors used to achieve the composite action between the GFRP cross section and the top concrete layer. Use of the 3-D woven material eliminates the delamination failure observed for some of the current commercially available GFRP bridge decks.

Introduction

The development of fiber reinforced composites for structural applications has grown significantly in recent years. The use of GFRP bridge decks is intended to provide a lightweight, corrosion resistant alternative to steel and concrete bridge deck. GFRP decks are

especially attractive in cases where decreasing the dead load, increasing the load ratings, or fast installation time is of high importance. Numerous manufacturers currently produce commercial GFRP bridge decking.

The cost of repairing or replacing deteriorated bridge infrastructure is very costly and warrants careful consideration. According to the most recent ASCE Infrastructure Report Card, the cost to eliminate current bridge deficiencies in the United States is \$9.4 billion a year for 20 years (2005). To many engineers, GFRP bridge decks seem to be an attractive option. However, several factors are currently slowing the widespread use of GFRP bridge decks. Some of these reasons include a high initial cost, a lack of design standards, and an unproven lifetime performance. According to Bakis et al., the most cost effective manufacturing process for producing GFRP bridge deck is using the pultrusion process (2002). This process involves drawing aligned fibers through a resin bath and shaping to the desired cross section.

Scope of Research

The research work presented in this paper explores an innovative GFRP bridge deck utilizing a three-dimensional weaving process. The scope of the project is exploratory in nature and is the first application of three-dimensional woven bridge deck with a constant cross section along the length of the deck. The advantage of the continuous cross section is that the length of deck can be produced for any desired length. The main goals of this pilot study were to design and fabricate a 3-D woven bridge deck, evaluate the structural performance, and sufficiently characterize the material components to allow accurate prediction of the material. In addition to the material property tests, a study of three types of shear connector configurations was conducted. Two types of bridge deck were fabricated and tested. The first type of bridge deck investigated the feasibility of a GFRP bridge deck without concrete topping. By using a GFRP-only bridge deck, the weight of the deck is typically reduced to 20 to 25 percent of an equivalent concrete deck. The second type of bridge deck investigated a hybrid GFRP/concrete bridge deck. This deck design includes the same type of GFRP panel used in the first design with shear connectors to ensure composite action between the GFRP and a thin concrete topping. The concrete topping serves a dual purpose in providing additional internal compression resistance and a suitable wearing surface to protect the GFRP from wear and exposure to weather conditions.

3-D Weaving Technology

Three dimensional woven composites have been investigated for various structural applications. The weaving process used in this research is shown in Fig. 1. The fabric contains three sets of yarns: the warp yarns in the x-direction parallel to the span of the deck, the filling yarns in the y-direction perpendicular to the warp yarns in the horizontal plane, and z-yarns which interlace both the x- and y-yarns in the vertical direction. The benefits of the three dimensional weaving process are the added fiber reinforcement which prevents delamination of the fibers observed in some unidirectional and bidirectional pultruded panels, as shown in Fig. 2. The vertical reinforcement strengthens the joints between the web and outer skins. Other benefits include increased out of plane performance, damage protection, and well-arranged fiber architecture. The improvement in the out-of-plane performance comes at the expense of slight decrease in the in-plane performance. The additional fibers in both the y- and z-directions decrease the stiffness of the deck as the percentage of fibers aligned in the span direction of the deck is reduced for an equal volume of GFRP.

Previous Work

The first investigation of 3-D GFRP decks was conducted by Norton (2004), by considering a “truss configuration” shown in Fig. 3. These decks consisted of three fabric skins; a top skin, a bottom skin, and a third diagonal skin which was stitched to the top and bottom skins at specified intervals. The deck was highly labor intensive to fabricate and could not be practically automated due to the continual insertion of the cores as the fabric was woven. In addition, the deck exhibited poor serviceability performance and was limited to incremental spans due to the presence of the diagonal fabric skins.

To address these concerns, this paper focuses on the behavior of a proposed second generation of 3-D woven bridge deck based on a “beam configuration.” This deck consists of two skins of E-glass fabric. Both skins consist of two layers of fabric woven together at continuous joints. One layer of both skins is cut along the joint and folded 90° to form a vertical web.

Fabrication of Test Specimens

A total of five deck panels were fabricated for this investigation. The design specifications and geometries for the GFRP-only decks and the hybrid decks are provided in Table 1 and Table 2, respectively. The fabrication process of the fabric preforms is illustrated in Fig. 4 (a) to (f). The first step of the fabrication process is the weaving of the E-glass fabric skins, one of which is shown in (a). Each deck consists of two skins of

fabric; both skins consist of two layers of fabric, giving a total of four layers of fabric per deck. One layer of each skin is cut parallel to the z-joint as shown in (b). This allows folding of this fabric at the joints, as shown in (c), to create completely vertical, full-height webs as shown in (d). Once all webs are cut, the top skin is inverted and placed atop the bottom skin as shown in (d), forming a modular bridge deck with full-height overlapping webs. Balsa wood cores were shaped to the cell openings between skins and included notches at each joint to account for the thickness of the joint as shown in (e). The excess fabric was trimmed after resin infusion, producing the final deck design as illustrated in (f). This is the extent of the fabric preform assembly for the three FRP-only decks, designated FRP1, FRP2, and FRP3, which are similar to the prototype deck shown in Fig. 5.

The additional two hybrid bridge decks, HYB1 and HYB2, required further assembly of shear connectors necessary to achieve the composite action between the GFRP decks and the concrete topping. HYB1 was tested with a short span of 1.22 m (4 ft) to emphasize the shear behavior due to flexure, while HYB2 had a relatively long span of 2.13 m (7 ft) to investigate the flexural behavior. The shear connectors were located at 90° from the direction of the deck span and covered the entire width of the deck. The shear connectors were placed on the top of the deck to ensure composite behavior of the FRP panel with a thin concrete overlay, as shown in Fig. 6. The shear connector fabric was woven identical to the deck fabric with the exception of the density of the yarns in the y-direction. The number of yarns in the y-direction was halved to economize the material usage, allow for easier shaping of the fabric, and to speed production.

After assembly of the fabric preforms, the decks were vacuum infused with an epoxy resin system. The panels were post cured the day after infusion in an oven for four hours in order to achieve maximum mechanical properties. The panels were trimmed to the final width of 0.46 m (18 in) to create a uniform specimen suitable for testing and modeling, neglecting edge effects.

The concrete topping of the hybrid panels was reinforced with a 6 mm (0.25 in) diameter steel wire mesh placed directly on top of the shear connectors. Five longitudinal bars were used in both decks and one transverse bar was placed on either side of each shear connector as shown in Fig. 7. Steel reinforcement was selected solely on availability and conventionality, but is not recommended for panels which will be exposed to the elements during the design life. The transverse reinforcement was placed in direct contact with the shear connectors to confine the concrete between shear connectors and provide some bearing on the FRP shear connectors. A 46 mm (1.8 in) thick concrete topping was cast over the top FRP skin to create a total deck

thickness of 163 mm (6.4 in). The concrete gradation was 78M, with a 3/8 in. nominal maximum size of aggregate. The small aggregate size was selected to allow the concrete to properly consolidate around the shear connectors.

Material Characteristics

The assemblage of the selected structural components for each bridge deck is a novel concept. The understanding and accurate prediction of the behavior of the bridge deck system as a whole is dependent upon accurate mechanical properties of each individual component. The authors made a concerted effort to characterize the GFRP, balsa, concrete, and steel materials used. The material property samples were cut from actual test decks. The testing performed on the GFRP skins included fiber volume fraction tests, four-point bending tests, tensile coupon tests, and compression coupon tests. One cell of the bridge deck was tested with the presence of the balsa to determine the compression characteristics of the deck. Concrete cylinders were tested in compression to determine the strength. The steel reinforcement was tested in tension. Two separate studies were performed. One was a resin study to compare two types of infusion systems. The second study was to investigate different types of shear connector configurations used to achieve composite action with the concrete topping.

The purpose of the GFRP fiber volume fraction test was to determine the E-glass fiber content of the skin layers. This quantity is useful for predicting the mechanical properties of the composite and is a strong indicator of the quality of resin infusion. The test was performed in accordance with ASTM D 3171-04. The volumes of sixteen GFRP skin specimens were measured prior to matrix burn-off. The specimens were placed in ceramic containers and heated in an oven for four hours at 400°C. The elevated temperatures ignited the cured thermosetting resin, leaving only the E-glass fabric. The mass of the remaining fabric was measured and converted to a volume using the known density of the E-glass. The average fiber volume fraction was 47% of the total skin volume, which is acceptable for vacuum infusion.

The tensile properties of the GFRP skins were determined in accordance with ASTM D 3039-06. The samples were 5 mm (0.2 in) thick x 25 mm (1.0 in) wide x 305 mm (12 in) long. Equal numbers of samples were cut from both the x- and y-directions. Aluminum tabs were attached to both ends of the samples to allow for adequate gripping. The change in gage length and load were recorded to develop the stress vs. strain curve for each specimen. The stress vs. strain relationship showed a strong linear relationship up to failure; the observed slight nonlinearity is attributed to cracking of the matrix.

The average modulus of elasticity was 23.65 GPa (3430 ksi) for the x-direction and 9.79 GPa (1420 ksi) for the y-direction. These values were very close to predictions based on the Rule of Mixtures, verifying the quality of weaving and infusion. The average tensile strength for the x-direction and y-direction samples was 510 MPa (74 ksi) and 69 MPa (10 ksi), respectively. These values were significantly lower than expected, which could be attributed to the observed premature failure within the grips due to excessive clamping.

Two tests were performed to evaluate the compression behavior of the GFRP material. The first test was similar to the tension test except for the loading direction and gage length, performed in accordance with ASTM D 3410-03. The samples were loaded in compression using a gage length of 12.7 mm (0.5 in) to prevent elastic buckling. Strain gages were attached to the samples to measure the axial strain. The purpose of this test was to determine the elastic modulus in compression, which was 11.85 GPa (1720 ksi) in the x-direction; however, buckling of the skins prevented accurate measurement of the compressive strength. Therefore, a second compression test was performed to determine the strength according to ASTM C 365. This test consisted of cutting a (0.5 in) thick slice of one cell of a GFRP-only deck. The balsa was left intact to provide lateral bracing for the GFRP skins. The contribution of the balsa was accounted for in determining the strength of the GFRP. The compressive strength of the GFRP in the x-direction was 193 MPa (28 ksi). The elastic modulus in compression is approximately half of the elastic modulus in tension due to the buckling of fibers when loaded in compression. The strength was also less than 50% of the tension test and was characterized by crushing of the matrix.

Four-point bending tests according to ASTM D 6272-02 were used to determine the flexural characteristics of the GFRP skin material. Samples from both x- and y-directions were tested. The specimens were 5 mm (0.2 in) thick, 25 mm (1.0 in) wide, and 127 mm (5.0 in) long. The specimens were tested using a simple span of 83 mm (3.25 in) and two loading points located at quarter-points of the span. The stress vs. strain relationship was developed and the elastic modulus was calculated from the initial portion of the curve from 0 to 20% of the ultimate strain. It should be noted that the stress and strain calculations in the ASTM standard are based on the assumption of equal strains at the top and bottom fibers. However, based on the tension and compression tests performed on the skins, the elastic modulus was highly dependent on the fiber direction. This suggests that the elastic modulus determined from bending should be between the bounds of the elastic modulus from tension and compression. The four-point bending test revealed an unanticipated behavior. The x-direction results are between the compression and

tension bounds and the y-direction results are not. The measured elastic modulus in the x-direction was 17.6 GPa (2550 ksi), which is lower than the value of 38.6 GPa (5600 ksi) measured in the y-direction. Although there are a larger percentage of fibers oriented in the x-direction, the placement of the fibers in the y-direction is above and below the x-yarns, providing a greater resistance to bending. In addition, the x-yarns provide additional resistance to bending in the y-direction as these fibers are densely packed.

The concrete properties were determined using ASTM C 39-05 and ASTM C 469-02 specifications. Thirteen 102 mm (4 in) x 203 mm (8 in) cylinders were loaded in compression to determine the stress vs. strain behavior using four linear motion transducers attached to metal rings with a known gage length. The elastic modulus of the concrete was 25 GPa (3630 ksi) and the average measured compressive strength was 58.6 GPa (8500 ksi).

The steel reinforcement used in the decks was also tested. The steel reinforcement was used for shrinkage reinforcement; however, the bars developed compressive stresses as the deck was loaded. The reinforcement was highly susceptible to buckling, preventing accurate measurements of the steel in compression. Therefore, tensile tests were performed to determine the elastic behavior and strength properties in accordance with ASTM A 370-05. The average elastic modulus was 216 GPa (31330 ksi) and the tensile strength was 593 MPa (86 ksi). The same values are assumed to apply for compression, citing the linear elastic isotropic nature of steel.

Resin Study

A separate study of was carried out to compare two types of resin infusion systems. The comparison of these two systems is not relevant to this paper, but did expose another advantage of the 3-D woven bridge deck. This study consisted of two sandwich panels formed with a balsa wood core sandwiched by two three-dimensionally woven fabric skins. The failure of both sandwich panels was initiated by buckling of the skins, which were not braced by the vertical webs present in the 3-D bridge decks. Therefore, the 3-D woven webs were shown to be necessary to eliminate the delamination of the skins. The epoxy panel exhibited a 14 percent higher stiffness and strength than the vinyl ester panel. However, the selected epoxy costs approximately double the vinyl ester for the same volume of cured resin. Therefore, the authors recommend considering vinyl ester for future research.

Shear Connector Investigation

The concept of a GFRP-concrete hybrid bridge deck assumes complete bond between the two materials. This bond allows transfer of the interfacial shear between the two materials as the deck is loaded. The quality of the bond for the proposed bridge deck is dependent on two main factors: size of the aggregate of the concrete mixture, surface texture of the top GFRP skin, and properly designed shear connectors. Ideally, this study would have been conducted prior to the fabrication of the deck specimens and used to aid the selection of shear connector type. However, time constraints and fabrication logistics required all test specimens to be fabricated simultaneously.

Three shear connector configurations were examined: a vertical flange shear connector (V), a rectangular wooden core (R), and a tapered core (T). The assembly of a tapered wooden core specimen is shown in Fig. 8. All shear connectors were designed with a height of 25 mm (1 in). The tapered core specimens were formed with two skins of 3-D woven fabric. These shear connectors flare out at the top, providing wedge action to confine the concrete. The rectangular core samples were identical to the tapered core, with the exception that the core inserts were a rectangular shape. This configuration was tested for its advantageous fabrication which avoided wrapping of the skin at sharp angles around the wooden core. Folding of the fabric skins becomes very difficult as the thickness of the fabric increases. However, yarns could be removed if necessary to facilitate folding. The third configuration consists of vertical flanges. No permanent wooden cores were used. This configuration was formed by folding one layer of fabric 90° upward to form vertical flanges. The fabrication of this configuration could be most easily mass produced using a reusable mold. These cores do not benefit from any wedge action, but allow for double the height of shear connectors at half the spacing of the other two configurations since no overlap of skins is necessary.

Testing of the shear connectors followed ASTM C 273 for shear testing of FRP sandwich panels. The goal was to simulate the shear interaction at the interface of the GFRP and concrete topping. The load was applied through two steel plates, one attached to the top of the concrete surface, the other to the GFRP skin as shown in Fig. 9. All nine specimens exhibited eventual debonding at the GFRP-concrete interface. The wooden core inserts acted as defects in the shear connectors as a soft point in the concrete topping. The vertical flange shear connector configuration achieved the highest stresses, as shown in Fig. 10, and benefited from rotations of the shear connectors. As the flanges rotated due to loading, the flanges were engaged in tension as opposed to pinching of the soft wood cores.

Behavior of the Bridge Deck

The deck specimens were tested in flexure. Each panel was loaded in three-point bending to examine the stiffness, ultimate flexural strength, and overall structural performance. The panels were loaded in increments of 8.9 kN (2,000 lb) up to 142 kN (32,000 lb) at a rate of 2.54 mm/min (0.1 in/min) and unloaded after each cycle to discern any permanent deformation. The selected load level of 32,000 lb corresponds to the AASHTO HS 30 equivalent wheel load including impact. The test setup is shown in Fig. 11. The final load cycle loaded the decks to failure.

The load was transferred from the actuator to the deck using a 102 mm (4 in) square hollow steel structural section across the entire width of the deck. The panels were simply supported at both ends by 51 mm (2 in) thick neoprene pads. The instrumentation of a typical deck is shown in Fig. 12. Each deck was instrumented with three potentiometers at the mid-span and one at either quarter-span to determine the deflection. One potentiometer was placed over each support to measure the compression of the neoprene pads. Strain gages were adhered to the top and bottom surfaces in both the span direction (x) and transverse direction (y). The measured deflections are compared to live load deflection limits for FRP bridge deck recommended by Williams et al. (2003), which range from L/360 to L/800.

The deflection of a flexural specimen is inversely proportional to the moment of inertia, I . In the case of a simply supported beam subjected to a point load at midspan, the deflection is given as:

$$\Delta = \frac{PL^3}{48EI} \quad [\text{Eq. 1}]$$

Furthermore, for rectangular shaped sections, the moment of inertia about the strong axis is:

$$I = \frac{bh^3}{12} \quad [\text{Eq. 2}]$$

where b is the width of the specimen and h is the height of the specimen. Eq. 2 shows that the moment of inertia is a linear function of the width. Therefore, substituting Eq. 2 into Eq. 1 shows that an increase in the width of a panel should inversely reduce the deflection. This ratio would not be accurate for very wide samples as b approaches infinity because only the portion of the panel near the load would be effective in transferring the load. Therefore, an “effective width” should be used to predict deflections of wide panels.

Due to width limitations of the selected weaving machine, the width of the decks produced is significantly less than the anticipated effective width provided by a

full-size panel. Due to the present lack of a design standard for GFRP bridge deck, the effective width for the panels is based on the AASHTO calculation for concrete decks. The equation for the effective width, w_d , in millimeters for a positive moment region is given as:

$$w_d = 660 + 0.55S \quad [\text{Eq. 3}]$$

where S is the spacing between supports and is measured in millimeters. The deflections are scaled assuming a linear reduction due to an increased effective width. The scaled deflections are listed for each panel at four prescribed AASHTO equivalent wheel load classifications. This consideration shows that the three FRP-only panels are at the threshold of satisfying recommended serviceability limits and the two hybrid panels are adequate for even the strictest serviceability recommendations. The scaled deflections are shown in Table 3 and Table 4.

GFRP Deck Behavior

All three GFRP deck panels exhibited a common failure mode: crushing of the top GFRP skin, as shown in Fig. 13. The amount of joint reinforcement between FRP1 and FRP2 showed to be a factor in the stiffness and failure mode. Failure of the z-yarns at the joints was evident for the FRP1 deck on the tension side at the midspan. The added reinforcement used in all other decks prevented joint failure prior to compression skin failure. The vertical shear webs were adequately designed to prevent buckling of the compression skins, eliminating the phenomenon observed in the first generation of 3D woven decks. The GFRP-only panels exhibited highly linear behavior to failure, as shown in Fig. 14. Cracking of the matrix was audible beginning at load levels of approximately 50% of the maximum load. The tension skin of each panel indicated no visual evidence of damage after failure of the compression skin. FRP3 exhibited no localized failures prior to brittle FRP compression failure as shown in the highly linear load vs. displacement relationship in Fig. 14. FRP3 was tested with a longer span than FRP1 and FRP2, and was less influenced by the shear contributions. After each unloading cycle, the GFRP panels exhibited no noticeable permanent deflection. Detailed results for each panel are given in Table 3.

Hybrid Panel Behavior

Neither of the hybrid panels exhibited noticeable permanent deformation prior to the failure cycle. The load vs. displacement relationship is shown for both panels in Figure 14. The two decks with a concrete topping failed due to failure of the concrete overlay. At 60% of the maximum load, slight cracking of the matrix was audible. The maximum load carried by the HYB1 panel was 300 kN (67,500 lb) causing shear failure of the

concrete as shown in Fig. 15. In addition, partial delamination of the concrete topping occurred on over half of the deck. Diagonal cracks in the concrete topping were also evident on the other end. The maximum measured strain in the concrete topping was 0.0034, which exceeded the failure strain specified by the concrete codes. Strains in the bottom GFRP skin reached approximately 10% of the failure strains, indicating a large reserve capacity. This panel performed more than adequately according to the specified guidelines for the live load deflection of L/800.

The clear span used for HYB 2 was 2.13 m (7 ft). The behavior of this panel was also highly linear up to the 142 kN (32,000 lb) cycle. The failure loading cycle exhibited three distinct peaks in loading. The first peak occurred at 190 kN (42,700 lb) at which point the concrete topping partially delaminated from one end. This delamination occurred at a net mid-span deflection of 30.2 mm (1.19 in). The second peak in loading occurred at 198 kN (44,500 lb) with a net mid-span deflection of 37.1 mm (1.46 in) and was marked by additional delamination of the concrete topping. The final peak in loading occurred at 205 kN (46,000 lb) with a deflection of 72.1 mm (2.84 in) at which the entire concrete topping on one end of the panel completely delaminated from the top FRP skin as shown in Fig. 16. Once the bond was completely broken, the sudden release of energy transferred the load solely to the shear connectors, failing four of the tapered skins in tension. The maximum measured compressive strain in the concrete was 0.002, while the maximum measured tensile strain in the GFRP was 0.0047. The higher values for the shorter span hybrid panel were not achieved due to the premature delamination of the concrete topping. Results for both of the hybrid panels are given in Table 4.

Analysis of Material Properties

The 3-D GFRP material has unique characteristics and, therefore, must be properly characterized for future design. The prediction of the 3-D GFRP material behavior presented in this paper is based on two analysis procedures: the principle of the Rule of Mixtures for composites and measured values from the four-point bending specimens.

Principle of the Rule of Mixtures

The Rule of Mixtures is a theory derived to provide a reasonable approximation of the elastic modulus in tension for uniaxial FRP. Since the material used in this program consists of fibers in three dimensions, the elastic modulus of the fibers, E_f , is reduced by 30 percent, which is proportional to the percentage of the fibers in the x-direction of 70% in comparison to the total amount of fibers.

The elastic modulus, E_x , in the x-direction in terms of the fiber volume fraction, V_f , the elastic modulus of the fibers, E_f , and the elastic modulus of the matrix, E_m , can be expressed as follows:

$$E_x = V_f E_f + (1 - V_f) E_m \quad [\text{Eq. 4}]$$

For the 3-D GFRP tested in this program, V_f is 0.47 based on the experimental results; E_f is 72.4 GPa (10,500 ksi); and E_m is 3.2 GPa (465 ksi), based on the manufacturer's data sheet. Therefore substituting into Eq. 4 gives,

$$\begin{aligned} E &= (0.47)(72.4)(0.7) + (0.53)(3.2) \quad [\text{Eq. 5}] \\ &= 25.5 \text{ GPa (3700 ksi)} \end{aligned}$$

The elastic modulus was evaluated based on coupon tests and found to be 23.7 GPa (3430 ksi) based on the tension test; 11.9 GPa (1720 ksi), based on the compression test; and 17.6 GPa (2550 ksi) based on the four-point flexure test.

This section presented an evaluation of the elastic modulus based on measured experimental values for the overall 3-D GFRP bridge decks and sandwich panels with different spans. The analysis from both categories provides consistent ranges for the elastic modulus that can be applied in future investigations of the 3-D GFRP material.

The analysis indicates that a conservative value of 19.3 GPa (2800 ksi) can be used for the elastic modulus of the new 3-D GFRP bridge decks with the specific design orientation of the fibers. This value also accounts for the balsa wood and the variation of the material properties of the top and bottom skins of the deck, due to the infusion process presented in this paper. It should be mentioned that the recommended value of E is approximately 70% of the value based on the principal of the Rule of Mixtures, due to the issues discussed above.

Elastic Modulus Based on Four-Point Bending Tests

The elastic modulus in flexure was evaluated based on the overall deflection of the four-point bending coupons. For a clear span, L , of 8.25 cm (3.25 inch), the elastic modulus can be evaluated based on the midspan deflection, Δ_t , in terms of the applied load, P , where b is the width of the coupon, a is the quarter-point ($a = L/4$) and d is the depth of the coupon, as follows:

$$\Delta_t = \frac{(P/2)(a)(3L^2 - 4a^2)}{24EI} \quad [\text{Eq. 6}]$$

Therefore, the elastic modulus can be determined based on the measured deflection, Δ_s , for a specified load, P , as:

$$E = \frac{5.9P}{\Delta_s bd^3} \quad [\text{Eq. 7}]$$

The limit of E was evaluated at different load values from 2.24 kN to 5.56 kN (0.5 to 1.25 kips) and was found to be from 13.3 to 15.0 GPa (1930 to 2170 ksi). The low values for E based on the four-point bending coupons could be due to shear stresses induced in the coupons due to the short span of 8.25 cm (3.25 inch) used in these tests.

Analysis of Decks

Four different approaches were investigated for predicting the deck behavior. The first approach analyzed the decks as simple beams. The second approach used a transformed section analysis to account for the assembly of heterogeneous materials. The first two approaches were verified using the third approach which was based on finite element analysis to account for more intricate modeling of the panels at the joints. All five deck specimens were analyzed. No distinction was drawn between FRP1 and FRP2, since they varied only in the amount of joint reinforcement. The selected loading condition for each deck was 20% of the maximum load. At this load level, the material components and the composite deck exhibit linear elastic behavior. These conditions are typical for predicting serviceability performance. The fourth approach was conducted to predict the elastic modulus of the three 3-D GFRP panels based on the measured deflection.

The first three approaches were investigated to predict the behavior of all five deck panels. For each approach, the selected loading condition was 20% of the maximum load. At this service load condition, the behavior of the material components is linearly elastic. The results of the first three analysis approaches are given in Table 5.

Method 1: Beam Analysis Approach

This approach was applied to all five deck panels and assumed a specified strain at the extreme compression face which was measured by a strain gage attached to the top surface of the deck specimens. Based on the assumption that plane sections remain plane during loading, a linear strain diagram is developed as shown in Fig. 17. The corresponding stresses are assumed to be linearly proportional to the strains to determine the internal moment capacity at the selected strain. This iterative process revealed that the neutral axis of the FRP-only panels was located below the mid-depth of the core material and for the hybrid panels was

located within the top GFRP skin. Using equilibrium and compatibility, the strain at the bottom of the GFRP tension skin was calculated and compared to the readings from the strain gages adhered to the surface. The differences in the strains were higher. This is attributed to the inaccurate assumption that plane sections remain plane which implies a linear strain distribution. The difference in the calculated internal moment and the applied moment matched more closely for the longer span decks. The percent difference between the predicted and measured values for the short span decks was typically double the percent difference for the longer span decks.

Method 2: Flexural Rigidity

This approach used the measured deflections to predict the overall flexural rigidity of deck panels. Both types of panels are naturally heterogeneous, since each consists of up to four materials: GFRP, balsa, steel, and concrete. Therefore, deflection equations derived from Bernoulli-Euler Beam Theory which assumes a homogeneous material cannot be applied directly. This approach uses a transformed section analysis which converts each material to an equivalent area of the balsa, which is the weakest material. This is accomplished by scaling the areas by the ratio of the elastic moduli of the materials to determine a transformed moment of inertia, I . Using the flexural rigidity, EI , for the deck cross-section, the deflections are predicted for the selected loading condition. This approach predicted deflections which were less than the measured values, suggesting the influence of shear deformation is significant. The shear deformation was accounted for using elementary sandwich theory (Allen 1969). The total deflection consists of two components: a portion due to bending and another portion due to shear. The total deflection is given as:

$$\Delta = \Delta_b + \Delta_s \quad [\text{Eq. 8}]$$

where

$$\Delta_b = \frac{PL^3}{48EI} \quad [\text{Eq. 9}]$$

$$\Delta_s = \frac{PL}{4AG} \quad [\text{Eq. 10}]$$

and

$$A = \frac{bd^2}{c} \quad [\text{Eq. 11}]$$

This approach is not directly applicable to the three-dimensionally woven decks, particularly for the hybrid panels, but is considered to be an approximation.

The depth c is the thickness of the core material, which is 102 mm (4 in) for both deck types. The distance d is defined as the distance between centerlines of the tension and compression skin areas. For the hybrid panels, the compression area includes the concrete and top GFRP skin and the tension skin is the entire bottom skin. Therefore, d is assumed to be the distance between the midpoints of these two zones. The shear modulus, G , defined by Allen should be that of the core material for sandwich panels since the face skins are relatively rigid in comparison. The shear modulus for the 3-D GFRP deck is based on estimated shear properties of the FRP webs and the balsa cores and is directly proportioned according to the volumes of both materials sandwiched between the top and bottom skins. The effective G for the core material of all deck panels was calculated as follows:

$$G = \frac{G_f A_f + G_b A_b}{A_f + A_b} \quad [\text{Eq. 12}]$$

where A_f is the area of the GFRP webs, G_f is the shear modulus of the GFRP, A_b is the area of the balsa wood cores, and G_b is the shear modulus of the balsa wood.

The inclusion of shear deformation increases the predicted deflections, but the percent difference from the measured values is still large. The predictions for the longer span panels very closely approximate the measured values with an average percent difference of 7%, but the shorter span predictions are much less than the measured values with an average percent difference of 41%. This suggests the effect of the shear deformation is more complex than can be accounted for using the above approximations.

Method 3: Finite Element Analysis

The final approach used to predict the overall deck behavior was using the finite element computer program ANSYS. The purposes of the finite element modeling were to compare to the other approaches and to more accurately represent the geometry at the joints, which cannot be easily captured by the first two approaches. The element type selected for all materials was SOLID185, an eight-noded brick with translational degrees of freedom at each node. In order to create a simple yet representative model of the actual deck, several key assumptions were made. These assumptions include:

- The shear connectors provide complete composite action. Therefore these tapered cores are not modeled to reduce the complexity. The topping is a solid slab of concrete 46 mm (1.8 in.) thick.

- To avoid using a nonlinear analysis and extensive testing on the neoprene pad supports beyond the scope of this exploratory project, the support conditions were modeled using antisymmetry boundary conditions assigned to the areas at the face of the support. This assumption prevents crushing of the deck at the support, which was not significant according to the experimental observations. Symmetry boundary conditions were applied to the areas at the mid-span and the load was applied uniformly over the appropriate contact area of the loading nose.
- The balsa cores do not contribute significantly to the stiffness of the deck. The primary function of the core inserts is to provide a formwork for the skins prior to infusion and prevent buckling of the skins. The elastic modulus of the balsa in the span direction is less than one percent of the next weakest material. The preliminary finite element model contained the balsa elements and showed minimal difference in performance, which justified this assumption.

The initial mesh consisted of elements typically measuring 25 mm (1 in.) along a side. The mesh size was halved for each subsequent analysis to a final element size of 6 mm (0.25 in.). At this point, the mid-span displacements converged to less than one percent of the previous mesh size. The percent differences between the 6mm (0.25 in) mesh size and the measured values from the experiment are given in Table 5. The results for the long span decks matched the experimental results very closely with a percent difference of 8.8%. The shorter decks were affected by shear deformation; therefore, the percent difference was 52%.

Method 4: Elastic Modulus of 3-D GFRP Decks

This section aims to evaluate the elastic modulus in flexure of the three 3-D GFRP bridge decks without concrete toppings based on the observed deflections. Elementary sandwich theory was applied for this analysis, which accounts for deflection due to both flexure and shear. This theory assumes a homogeneous core, which is not the case for the 3-D GFRP decks which consist of balsa and GFRP. Therefore, three limits for the elastic modulus in flexure were evaluated for each bridge deck. The upper limit is evaluated by considering the shear deflection component due to the contribution of the balsa wood to the core. This limit provides a low value for the shear rigidity of the deck and therefore results in a high value for the shear deflection component. Therefore, for a measured deck deflection, this limit results in a low value for the flexure deflection component and therefore, an upper limit for E . For the 122 cm (48 inch) span deck, the upper limit can be

evaluated, in terms of the applied load, P , and the total deflection, Δ_t , as follows:

$$\Delta_t = \Delta_b + \Delta_s \quad [\text{Eq. 13}]$$

where

$$\Delta_t = \frac{PL^3}{48EI} + \frac{PL}{4U}; U \text{ is the panel shear rigidity} \quad [\text{Eq. 14}]$$

$$U = \frac{G(d+c)^2 b}{4c}, \text{ in N (kips)}. \quad [\text{Eq. 15}]$$

where G is the shear modulus of the core material (1.0 GPa for the balsa and 10.6 GPa for the GFRP webs); d is the total depth of the panel (112 mm); c is the depth of the core (102 mm); and b is the width of the panel (416.6 mm for the balsa and 40.6 mm for the GFRP webs).

Using the above values yields the following expression for the elastic modulus, E :

$$E = \frac{51.88P}{\Delta_t - 0.0118P} \quad [\text{Eq. 16}]$$

All the limits were evaluated at different load levels from 89 to 133 kN (20 to 30 kips). This range was selected to be within the elastic region of the materials as shown in the material property tests.

The intermediate limit can be evaluated by using the shear deflection component due to only the 3-D GFRP. In this case, the corresponding shear rigidity of the deck is much higher than in the first case and, therefore, provides a low value for the shear contribution to the deflection. For a given measured value of the total deflection, this limit results in an intermediate value for the flexure deflection component and, therefore, an intermediate limit for E . For the 122 cm (48 inch) span deck, the intermediate limit can be evaluated, in terms of the applied load, and the total deflection, as follows:

$$\Delta_t = \frac{PL^3}{48EI} + \frac{PL}{4U} \quad [\text{Eq. 17}]$$

using

$$G = \frac{E}{2(1+0.12)} = \frac{E}{2.24} \quad [\text{Eq. 18}]$$

$$U = 3.15 E \quad [\text{Eq. 19}]$$

The elastic modulus can be determined for the load level, P , and corresponding deflection, Δ_t , as:

$$E = \frac{55.69P}{\Delta_t} \quad [\text{Eq. 20}]$$

The lower limit for the elastic modulus of the decks can be evaluated by using the shear deflection component due to both the 3-D GFRP and the balsa wood. In this case, an approximate value for the shear modulus of the core was used in proportional to the width of each material. This limit provides the highest shear rigidity, which predicts the lowest shear deflection. Therefore, for a given measured value of the total deflection, this limit results in the highest value for the flexure deflection component and therefore, a lower limit for E .

For the 120 cm (48 inch) span deck, the lower limit can be evaluated in terms of the applied load and the total deflection as follows:

$$G = G_{3-D \text{ GFRP}} \times \frac{A_f}{A_f + A_b} + G_{balsa} \times \frac{A_b}{A_f + A_b} \quad [\text{Eq. 21}]$$

$$G = 10.57 \times \frac{40.6}{457.2} + 0.014 \times \frac{416.6}{457.2} \quad [\text{Eq. 22}]$$

$$= 1.027 \text{ GPa (149 ksi)}$$

using the total deflection, Δ_t , as:

$$\Delta_t = \frac{PL^3}{48EI} + \frac{PL}{4U} \quad [\text{Eq. 23}]$$

and

$$U = \frac{(1.027)(213.3^2)(457.2)}{(4)(101.6)} \quad [\text{Eq. 24}]$$

$$= 52,570 \text{ kN (11,800 kips)}$$

The elastic modulus can be evaluated for a specified load level, P , and corresponding Δ_t , as:

$$E = \frac{51.88P}{\Delta_t - 0.00101P} \quad [\text{Eq. 25}]$$

It was noticed that the intermediate limits and the lower limits are very close since the contribution of the balsa wood to the stiffness is negligible. The ranges for each limit for all the decks are presented in Table 1. Based on the analysis of this section, the lower limit of E is believed to provide a better approximation since it accounts for the 3-D GFRP webs and the balsa wood.

Conclusions and Future Work

This pilot study was successful in incorporating many structural components into a high performance bridge deck given limited resources and restricted design flexibility. Modifications to the fabrication process will be required for efficient production. Nevertheless, this pilot study concluded the following major findings:

1. The use of the 3-D weaving process eliminated the failure mode of fiber delamination at the joints common in current bridge decks.
2. The vacuum infusion process and post curing process were highly labor intensive. Optimization of the fabrication process was far beyond the scope of this pilot study, but use of resins which cure at ambient conditions and use of wet-out processes similar to pultrusion could drastically increase productivity.
3. The bond between the concrete and GFRP was inadequate for the hybrid panels. Roughening of the GFRP surface or use of a bonding agent would have increased the strength of the hybrid decks by 50%. This projected increase is based on the measured strain in the concrete from the deck tests reaching the ultimate strain measured in the concrete from the cylinder tests.
4. Simple analysis procedures are accurate to provide a baseline prediction for 3-D woven decks, especially for longer spans typical of bridge decks. For shorter span decks, the behavior is complicated by stronger influence of shear deformation, which was beyond the scope of this pilot investigation. Further insight into the shear behavior of the decks could be obtained by performing shear tests on the GFRP-only panels using ASTM C 273.
5. With a limited skin thickness and depth of the deck, the performance of these hybrid panels was shown to be adequate for AASHTO truck load classifications. More extensive testing will be necessary to ensure reliability for commercial production. Unlike other currently produced decks, the fiber architecture of this design can be tailored during the weaving process to eliminate other failure modes, such as punching shear commonly exhibited in other FRP decks. The GFRP-only panels were about 50% of the stiffness and weight of the hybrid panels.
6. The shear connectors which are most suited for 3-D GFRP decks were the vertical flange shear connectors. A possible variation on this design for future research is a vertical flange folded at the top to create a head similar to Nelson shear studs designed for composite action on steel beams.

Acknowledgments

The authors would like to acknowledge the financial support by the National Science Foundation grant CMS-0301233. The authors are also appreciative for the partnership with 3TEX, Inc. in the weaving and fabrication of the test specimens for this project.

References

- 3TEX, Inc. (2004) "96 oz 3Weave™ E-Glass 2022 Silane Sized Product Data Sheet." <<http://www.3tex.com/uploadedfiles/P3W-GE044.pdf>>.
- AASHTO. (2004) *AASHTO LRFD Bridge Design Specifications*. 3rd ed. American Association of State Highway and Transportation Officials.
- ASCE (2005) "Report Card for America's Infrastructure." <<http://www.asce.org/reportcard>>.
- Bakis, C., Bank, L., Brown, V., Cosenza, E., Davalos, J., Lesko, J., Machida, A., Rizkalla, S., Triantafillou, T. (2002) "Fiber-Reinforced Polymer Composites for Construction—State-of-the-Art Review." *Journal of Composites for Construction*, May.
- Johnson, C. (2006) "Fabrication and Behavior of Three-Dimensionally Orthogonal Woven FRP/Concrete Bridge Deck." Masters Thesis, North Carolina State University.
- Mohamed, T. (2006) "Fabrication and Behavior of Three Dimensionally Woven GFRP Bridge Deck." Masters Thesis, North Carolina State University.
- Norton, T. (2004) "3D Orthogonal Woven GFRP Bridge Deck: Fabrication and Experimental Investigation." Masters Thesis, North Carolina State University.

Table 1. Deck specs for 3-D GFRP panels.

	FRP1	FRP2	FRP3
Design	102 mm (4 in.) vertical webs with balsa cores 6 z-yarns per joint	102 mm (4 in.) vertical webs with balsa cores 12 z-yarns per joint	102 mm (4 in.) vertical webs with balsa cores 12 z-yarns per joint
Specs	Span: 1.22 m (48 in.) Width: 0.46 m (18 in.) Depth: 112 mm (4.4 in.) composite	Span: 1.22 m (48 in.) Width: 0.46 m (18 in.) Depth: 112 mm (4.4 in.) composite	Span: 2.13 m (84 in.) Width: 0.46 m (18 in.) Depth: 112 mm (4.4 in.) composite
Shear Connectors	none	none	none

Table 2. Deck specifications for hybrid panels.

	HYB1	HYB2
Design	102 mm (4 in.) vertical webs with balsa cores 12 z-yarns per joint	102 mm (4 in.) vertical webs with balsa cores 12 z-yarns per joint
Specs	Span: 1.22 m (48 in.) Width: 0.46 m (18 in.) Depth: 112 mm (4.4 in.) composite + 5 mm (0.2 in) shear connector skin + 46 mm (1.8 in.) concrete	Span: 2.13 m (84 in.) Width: 0.46 m (18 in.) Depth: 112 mm (4.4 in.) composite + 5 mm (0.2 in) shear connector skin + 46 mm (1.8 in.) concrete
Shear Connectors	25 mm (1 in.) tapered 3D woven GFRP with core inserts	25 mm (1 in.) tapered 3D woven GFRP with core inserts

Table 3. Test results for 3-D GFRP panels.

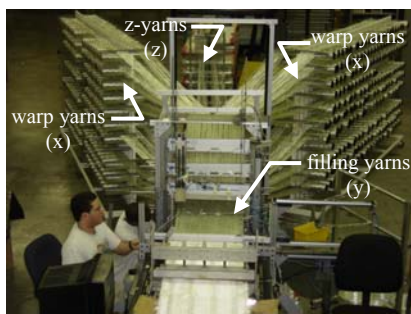
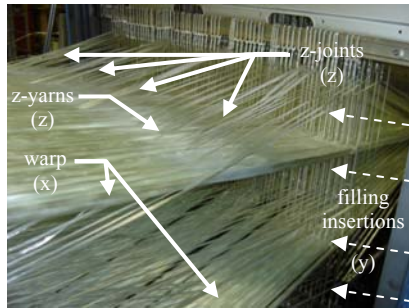
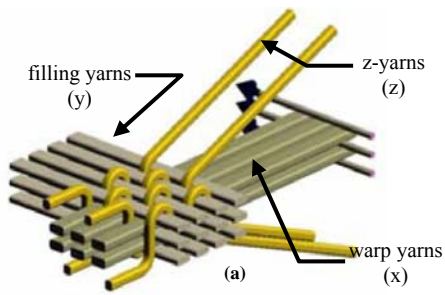
	FRP1	FRP2	FRP3
Service Load Deflection	13.85 mm (0.545 in)	5.89 mm (0.232 in)	15.86 mm (0.624 in)
20% Max Load	L/88	L/207	L/135
Effective Width	331 mm (52 in)	331 mm (52 in)	834 mm (72 in)
Service Load Deflections Scaled for Effective Width 20% Max Load	4.78 mm (0.188 in) L/255	2.03 mm (0.08 in) L/600	3.95 mm (0.156 in) L/540
Effective HS 15 Deflection	L/283	L/335	L/230
Effective HS 20 Deflection	L/212	L/249	L/167
Effective HS 25 Deflection	L/181	L/212	L/141
Effective HS 30 Deflection	L/140	L/170	L/110
Failure Load	153 kN (34,300 lb)	188 kN (42,300 lb)	145 kN (32,600 lb)
Failure Mode	GFRP compression failure, z-joint failure	GFRP compression failure	GFRP compression failure

Table 4. Test results for hybrid panels.

	HYB1	HYB2
Service Load Deflection	2.76 mm (0.109 in)	5.74 mm (0.226 in)
20% Max Load	L/442	L/372
Effective Width	331 mm (52 in)	834 mm (72 in)
Service Load Deflections Scaled for Effective Width 20% Max Load	0.95 mm (0.038 in) L/1270	1.43 mm (0.056 in) L/1490
Effective HS 15 Deflection	L/899	L/838
Effective HS 20 Deflection	L/757	L/610
Effective HS 25 Deflection	L/638	L/513
Effective HS 30 Deflection	L/508	L/425
Failure Load	300 kN (67,500 lb)	205 kN (46,000 lb)
Failure Mode	Concrete shear failure	Progressive delamination of concrete topping, tension failure of FRP shear connectors

Table 5. Predictions based on analytical approaches.

	FRP1	FRP2	FRP3	HYB1	HYB2
Beam Analysis Percent Difference	31.6%	15.6%	13.5%	16.0%	9.9%
Flexural Rigidity Percent Difference	77.4%	34.5%	1.3%	44.8%	11.8%
Finite Element Percent Difference	79.0%	39.0%	11.7%	36.5%	5.9%



(b)

(c)

Figure – 1 (a) Orthogonal weaving process by 3TEX (2004); (b) fiber orientation in decks; (c) setup of entire weaving process.



Figure – 2 Fiber delamination at joints of unidirectionally pultruded panels.

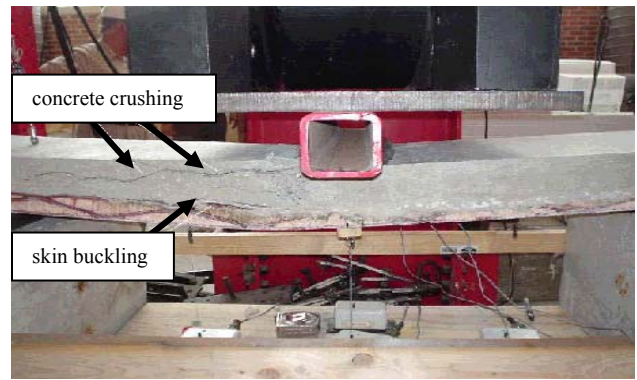


Figure – 3 Failure of 1st generation 3-D GFRP panel by Norton (2004).

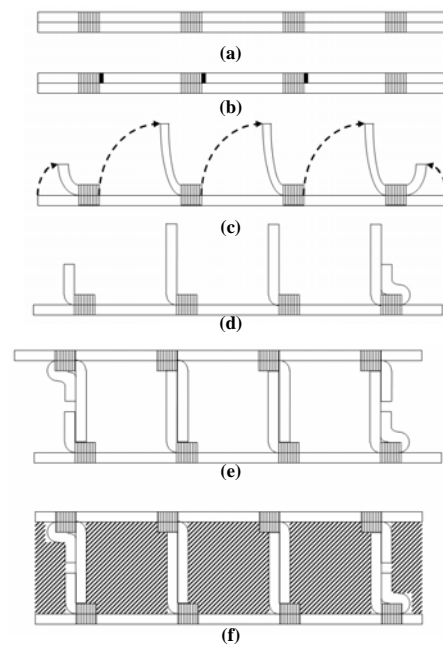


Figure – 4 Assembly of FRP-only panels. (a) produce woven skin; (b) cut one layer of skin at z-joint; (c) fold fabric upwards; (d) form half of full-depth overlapping webs; (e) invert identical top skin and place atop bottom skin; (f) insert balsa cores and trim excess fabric.



Figure – 5 Prototype 2nd generation 3-D GFRP deck with constant cross section.

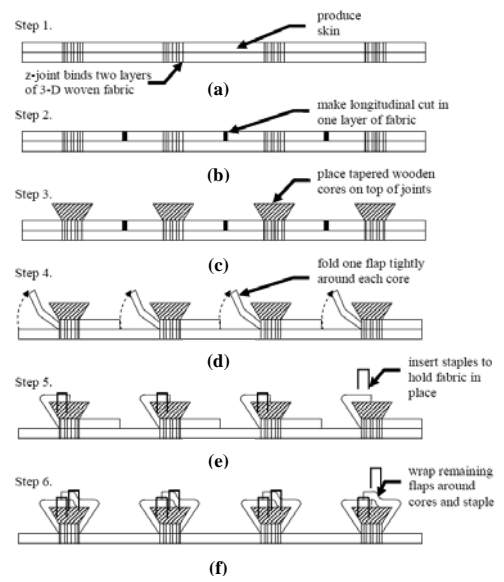


Figure – 8 Shear connector assembly.

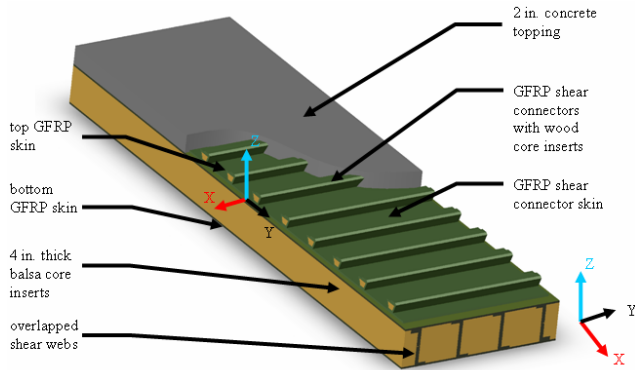


Figure – 6 Schematic of GFRP/concrete hybrid panels.



Figure – 9 Shear connector failure.

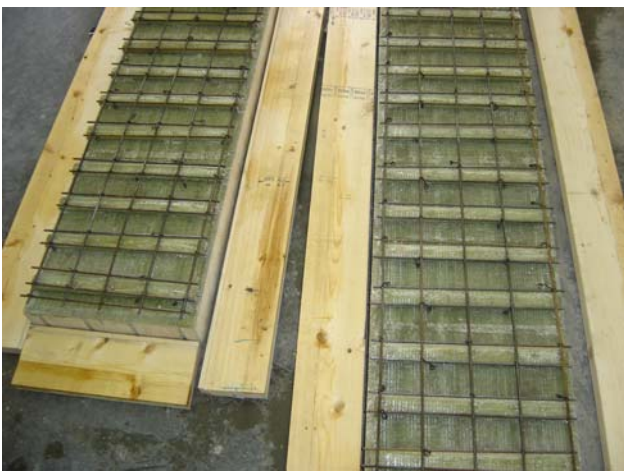


Figure – 7 Steel mesh reinforcement in hybrid panels.

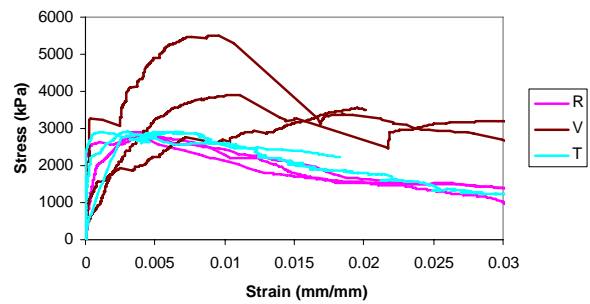


Figure – 10 Shear connector study test results.



Figure – 11 Three-point bending test setup of FRP3.

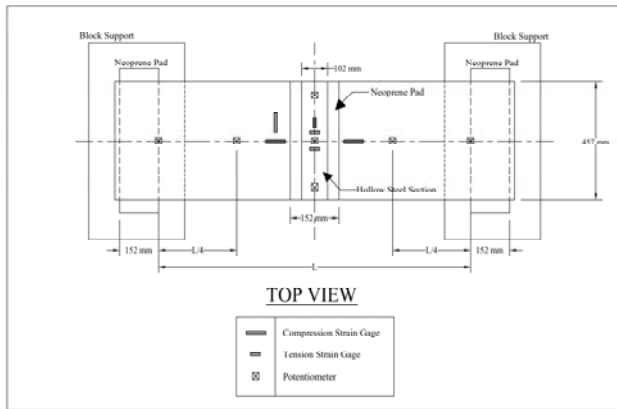


Figure – 12 Instrumentation of typical deck panel.

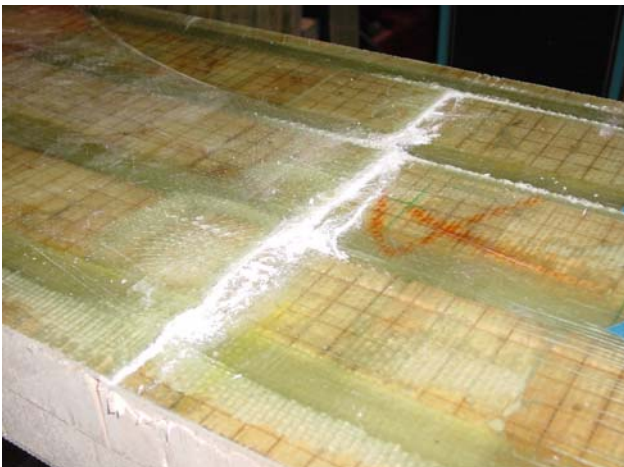


Figure – 13 Typical compression skin failure mode of FRP-only panels.

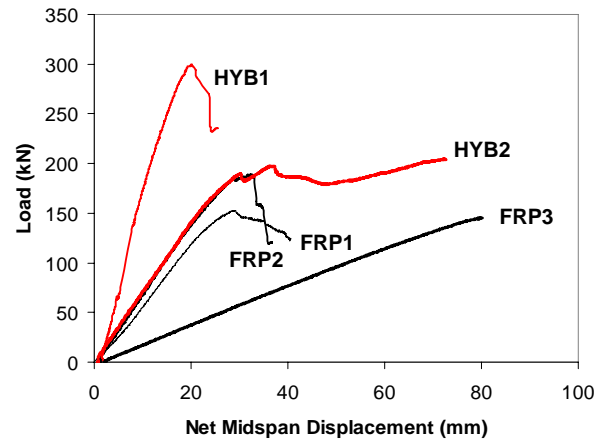


Figure – 14 Load vs. Displacement for all deck panels.

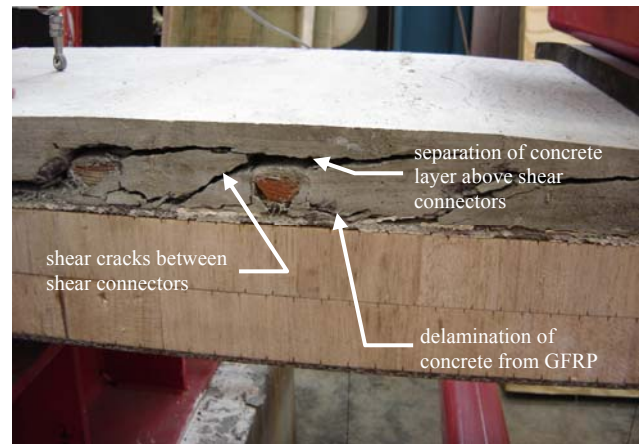


Figure – 15 Failure of concrete topping on HYB1.

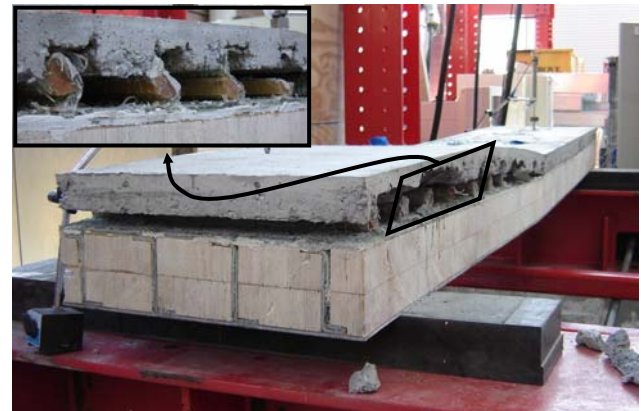
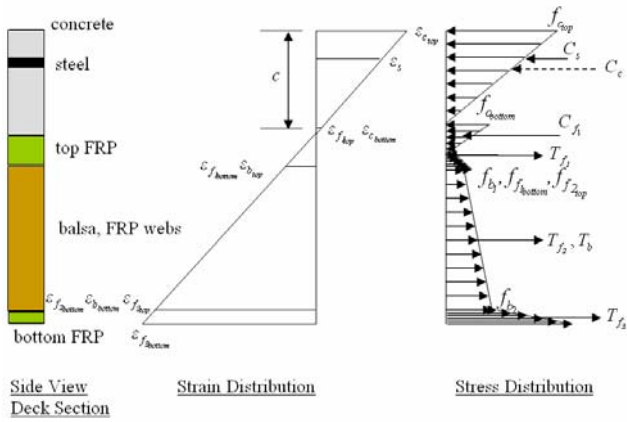


Figure – 16 Delamination of concrete topping on HYB2.



Authors:

Charles M. Johnson, NC, North Carolina State Univ.
 Master of Science Student
 Consultant at City Structures D&P, Lewisville, NC

Tarek S. Mohamed, CA, North Carolina State Univ.
 Master of Science Student
 Design Division of L.A. County Public Works, CA

Sami H. Rizkalla, NC, North Carolina State Univ.
 Distinguished Professor
 Director of Constructed Facilities Lab, Raleigh, NC

Figure – 17 Stress and strain distributions over hybrid deck cross sections.